

A crossed beam investigation of the reactions of tricarbon molecules, $C_3(X^1\Sigma_g^+)$, with acetylene, $C_2H_2(X^1\Sigma_g^+)$, ethylene, $C_2H_4(X^1A_g)$, and benzene, $C_6H_6(X^1A_{1g})$

Xibin Gu ^a, Ying Guo ^a, Alexander M. Mebel ^b, Ralf I. Kaiser ^{a,*}

^a Department of Chemistry, University of Hawai'i at Manoa, Honolulu, HI 96822, United States

^b Department of Chemistry and Biochemistry, Florida International University, Miami, FL 33199, United States

Received 26 July 2007; in final form 10 October 2007

Available online 13 October 2007

Abstract

Crossed molecular beams experiments have been conducted to examine the chemical dynamics of the reactions of the tricarbon molecule, $C_3(X^1\Sigma_g^+)$, with acetylene, $C_2H_2(X^1\Sigma_g^+)$, ethylene, $C_2H_4(X^1A_g)$, and benzene, $C_6H_6(X^1A_{1g})$. All reactions proceeded via a tricarbon versus atomic hydrogen exchange pathway and are defined by characteristic threshold energies of 80–90 kJ mol⁻¹ (acetylene), 40–50 kJ mol⁻¹ (ethylene), and 90–110 kJ mol⁻¹ (benzene) yielding the 2,4-pentadiynylidyne radical, HCCCCC($X^2\Pi$) (acetylene), 1,2,3,4-pentatetraene-yl-1, HCCCCCH₂(X^2B_1) (ethylene), and phenyltricarbon, C₆H₅CCC(X^2A) (benzene) plus atomic hydrogen. Our findings suggest that tricarbon molecules can react in high temperature combustion flames with unsaturated hydrocarbon molecules to form hydrogen-deficient radicals.

Published by Elsevier B.V.

1. Introduction

The energetics and dynamics of the reactions of small carbon molecules are of paramount importance in understanding combustion processes [1] and the chemical vapor deposition of diamonds [2]. Particular attention has been devoted to understand the reactions of small carbon molecules and to incorporate these data into combustion and chemical vapor deposition models. Dicarbon and tricarbon are the simplest representatives of bare carbon molecules. Both species have been identified in high temperature combustion flames under fuel-rich conditions of incipient soot formation at concentrations near 10¹⁵ cm⁻³ [3]. Reactions of dicarbon and tricarbon are also important in chemical vapor deposition processes of nano diamonds [4]. Although current models favor the methyl radical as the

key growth species in low power reactors [5], recent spectroscopic investigations of CVD environments detected dicarbon molecules via laser induced fluorescence. More complex species such as diacetylene (C₄H₂), C₄H₃ isomers, and vinylacetylene (C₄H₄) of hitherto unknown origin were further identified in diamond formation processes [6]. These processes are closely related to the growth of carbon clusters in carbon-rich stars as well as to the synthesis of diamonds in hydrogen-poor preplanetary nebulae. Due to the importance of dicarbon and tricarbon reactions, the kinetics of these species have been extensively investigated. In these studies, the disappearance of, for instance, dicarbon in both the singlet ground state and the electronically excited triplet state was followed. The reactions of C₂($X^1\Sigma_g^+$) were found to be fast (of the gas kinetic order with rate constants of a few 10⁻¹⁰ cm³ s⁻¹ when the molecular partner is an unsaturated hydrocarbon), whereas the C₂($a^3\Pi_u$) reactions were suggested to be systematically slower. Rate constants of C₃($X^1\Sigma_g^+$) reactions with unsaturated hydrocarbons have been tackled, too. They were

* Corresponding author. Fax: +1 808 9565908.

E-mail address: xibin@hawaii.edu (X. Gu).

found to be steadily smaller than the related reactions of dicarbon and seldom reached $10^{-12} \text{ cm}^3 \text{ s}^{-1}$ at room temperature [7]. This suggested the existence of characteristic threshold energies [8].

However, information on the reaction products is still missing. How can these be identified? Crossed molecular beams experiments [9–11] have played an important role in accessing the relevant regions of the potential energy surfaces of important combustion intermediates and in elucidating possible reaction pathways how they might be formed in combustion flames. The experimental dynamics of the tricarbon molecule have only been exposed with methylacetylene and allene as a co-reagent [12]. In the present Letter, we portray crossed molecular beams studies of the tricarbon molecule, $\text{C}_3(\text{X}^1\Sigma_g^+)$, with acetylene, $\text{C}_2\text{H}_2(\text{X}^1\Sigma_g^+)$, ethylene, $\text{C}_2\text{H}_4(\text{X}^1\text{A}_g)$, and benzene, $\text{C}_6\text{H}_6(\text{X}^1\text{A}_{1g})$.

2. Experimental

The experiments were carried out under single collision conditions in a crossed molecular beams machine at The University of Hawaii [13,14]. Pulsed tricarbon beams were produced in the primary source by laser ablation of graphite at 266 nm [15] (8–30 mJ per pulse; Table 1). Under these conditions, no carbon clusters higher than tricarbon are present in the primary beam. The ablated species were seeded in neat carrier gas (helium, 99.9999%, Airgas) released by a Proch-Trickl pulsed valve. A four-slot chopper wheel mounted between the skimmer and the cold shield selected a part out of the seeded tricarbon beam [16]. This segment of the tricarbon beam crossed a pulsed hydrocarbon beam of acetylene (99.9%; Airgas), ethylene (99.999%; Airgas), neon-seeded (about 5%) benzene (+99%, Aldrich) released by a second pulsed valve in the interaction region of the scattering chamber. The reactively scattered species are monitored using a triply differentially pumped quadrupole mass spectrometric detector (QMS) in the time-of-flight (TOF) mode after electron-impact ionization of the neutral molecules. The detector can be rotated within the plane defined by the primary and the secondary reactant beams to allow taking angular resolved TOF spectra. By integrating the TOF spectra at distinct laboratory angles, we obtain the laboratory angular distribution, i.e.,

the integrated signal intensity of an ion of distinct m/z versus the laboratory angle. Information on the chemical dynamics was obtained by fitting these TOF spectra of the reactively scattered products and the product angular distribution in the laboratory frame (LAB) using a forward-convolution routine [17]. This procedure initially guesses an angular distribution $T(\theta)$ and a translational energy distribution $P(E_T)$ in the center-of-mass reference frame (CM). TOF spectra and the laboratory angular distribution were then computed from the initial trial functions, $T(\theta)$ and $P(E_T)$. Best fits of the TOF and laboratory angular distributions were achieved by refining the $T(\theta)$ and $P(E_T)$ parameters. Since the reactions of tricarbon molecules with unsaturated hydrocarbons have characteristic threshold energies, E_0 [18], we utilized an energy dependent cross section, σ , via the line-of-center model through Eq. (1) with the collision energy E_C for $E_C \geq E_0$ in the fitting routine.

$$\sigma \sim [1 - E_0/E_C] \quad (1)$$

3. Results

3.1. Laboratory data

3.1.1. $\text{C}_3/\text{C}_2\text{H}_2$ system

We detected reactive scattering signal at $m/z = 61$ (C_5H^+) and 60 (C_5^+). However, at each laboratory angle, the TOF spectra at both mass-to-charge-ratios are – after scaling – identical. This finding alone leads us to two conclusions. First, ions at $m/z = 60$ originate from dissociative ionization of the C_5H neutral radical in the electron impact ionizer. Secondly, only the tricarbon versus atomic hydrogen reaction to form C_5H radical(s) is open, but not the molecular hydrogen elimination channel (Fig. 1a). However, for TOF spectra of ions recorded at lower mass-to-charge ratios such as of 49 (C_4H^+), 48 (C_4^+), 37 (C_3H^+), and 36 (C_3^+), the situation is more complex [19]. These ions originated from dissociative ionization of the C_5H parent at $m/z = 49, 48, 37, 36$, from the ionized C_4H parent molecule formed in reaction of co-ablated dicarbon molecules with acetylene ($m/z = 49$), from dissociative ionization of the C_4H parent ($m/z = 48, 37, 36$), and from the ionized C_3H parent molecule formed in reaction of co-ablated carbon atoms with acetylene [20]. Signal at $m/z = 36$ (C_3^+) has contributions from (i) dissociative ionization of the C_5H , C_4H , and C_3H parents, (ii) reactive scattering signal of the carbon atom versus molecular hydrogen exchange in the carbon–acetylene reaction [19], and – for those TOFs taken close to the primary beam – from inelastically scattered tricarbon molecules. The corresponding LAB distribution of the ions at $m/z = 61$ is very narrow and extends only by about 15° in the scattering plane defined by both beams (Fig. 1b); TOF could not be recorded at angles of less than 4° with respect to the primary source beam due to the enhanced helium gas load at angles in close proximity to the beam.

Table 1
Peak velocities (v_p), speed ratios (S) and the center-of-mass angles (θ_{CM}), together with the nominal collision energies (E_C) of the tricarbon–acetylene, ethylene, and benzene systems

Beam	v_p (ms^{-1})	S	E_C (kJ mol^{-1})	θ_{CM}
$\text{C}_2\text{H}_2(\text{X}^1\Sigma_g^+)$	902 ± 2	16.0 ± 1.0	–	–
$\text{C}_3(\text{X}^1\Sigma_g^+)$	4018 ± 122	1.5 ± 0.1	128 ± 8	9.2 ± 0.3
$\text{C}_2\text{H}_4(\text{X}^1\text{A}_g)$	893 ± 3	15.7 ± 1.0	–	–
$\text{C}_3(\text{X}^1\Sigma_g^+)$	2899 ± 113	2.7 ± 0.3	73 ± 5	13.4 ± 0.5
$\text{C}_6\text{H}_6(\text{X}^1\text{A}_{1g})$	762 ± 3	21.6 ± 1.0	–	–
$\text{C}_3(\text{X}^1\Sigma_g^+)$	3680 ± 153	1.8 ± 0.2	174 ± 14	24.2 ± 1.0

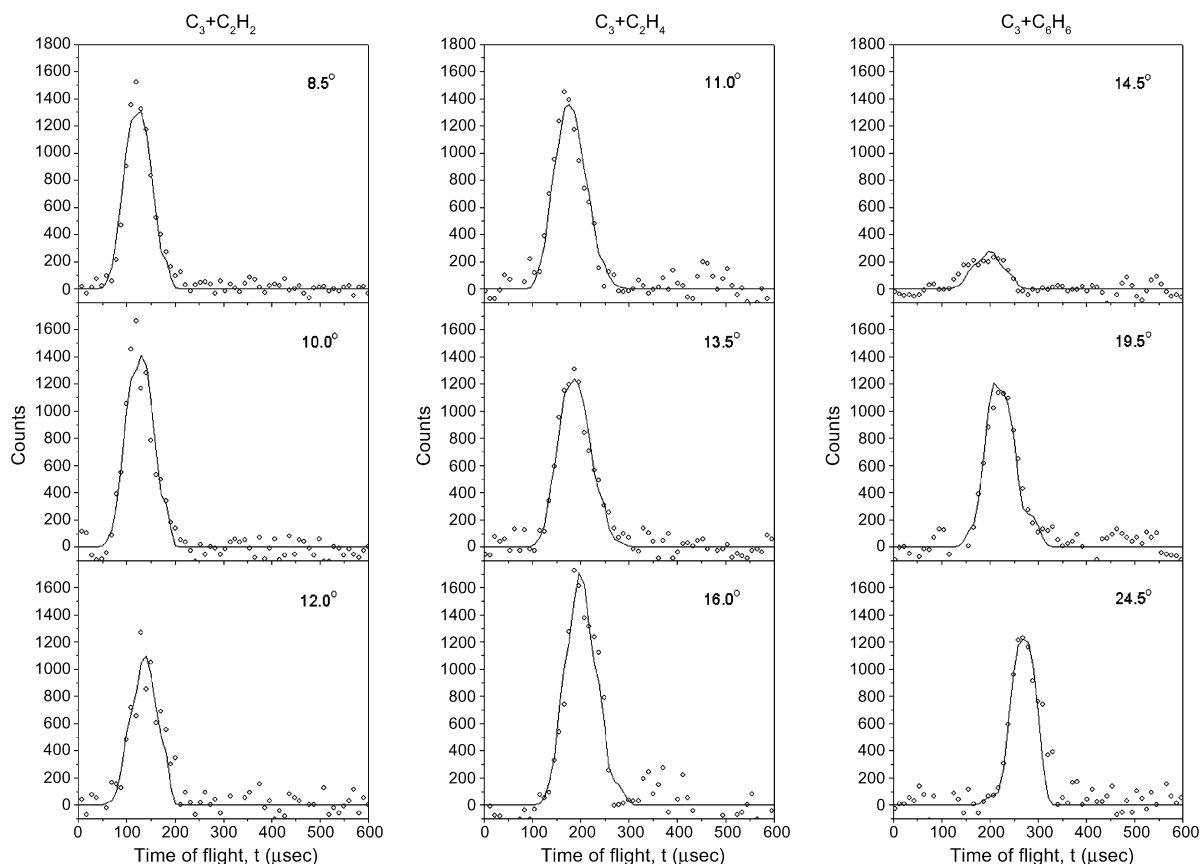


Fig. 1a. Selected time-of-flight data for $m/z = 61$ (C_5H^+), $m/z = 63$ ($C_5H_3^+$) and $m/z = 113$ ($C_9H_5^+$) recorded for the reactions of tricarbon molecules with acetylene (left), ethylene (center) and benzene (right) and at various laboratory angles. The circles indicate the experimental data, the solid lines the calculated fit.

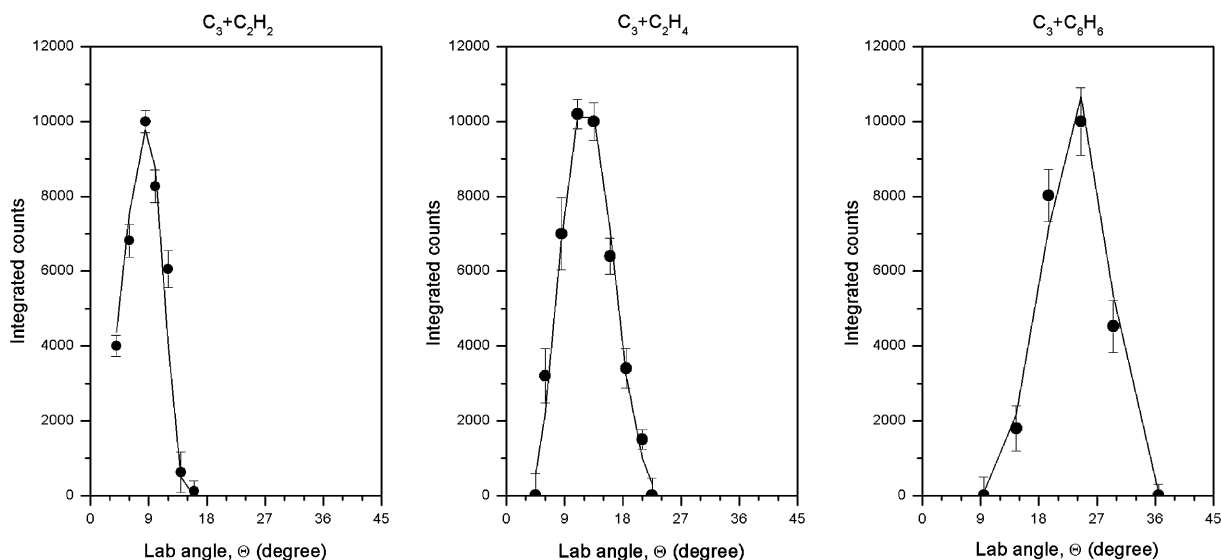


Fig. 1b. Laboratory angular distribution of the C_5H , C_5H_3 , C_9H_5 radical products recorded at $m/z = 61$, $m/z = 63$, and $m/z = 113$ for the reactions of tricarbon with acetylene (left), ethylene (center) and benzene (right). Circles and error bars indicate experimental data, the solid line the calculated distribution with the best-fit center-of-mass functions.

3.1.2. C_3/C_2H_4 system

In case of the tricarbon–ethylene system, signal was detected at $m/z = 63$ ($C_5H_3^+$), 62 ($C_5H_2^+$), 61 (C_5H^+),

and 60 (C_5^+). Ion counts at lower mass to charge ratios originate in dissociative ionization of the parent molecule – here C_5H_3 – in the electron impact ionizer of the detector.

Therefore, the tricarbon versus atomic hydrogen pathway is open (Fig. 1). We also monitored ion counts at lower mass-to-charge ratios of 51 ($C_4H_3^+$), 50 ($C_4H_2^+$), 49 (C_4H^+), 48 (C_4^+), 39 ($C_3H_3^+$), 38 ($C_3H_2^+$), 37 (C_3H^+), and 36 (C_3^+) [19]. They result from dissociative ionization of the C_5H_3 parent molecules, from ionization of the *i*- C_4H_3 ($m/z = 51$) radical formed in the reaction of dicarbon with ethylene [21], and from ionization of the propargyl radical, $C_3H_3(X^2B_1)$, synthesized in the carbon atom–ethylene reaction ($m/z = 39$). Within the experimental signal-to-noise ratio, no other channels were observed. These parent species also fragment in the electron impact ionizer to give signal at $m/z = 50$ –48 and 38–36. Finally, we also have to account for an elastic scattering of the tricarbon molecule with ethylene at angles close to the primary beam for $m/z = 36$. Similarly to the acetylene reactant, the laboratory angular distribution of ions at $m/z = 63$ is narrow and spread over only 25° in the scattering plane (Fig. 1b).

3.1.3. C_3/C_6H_6 system

Considering the tricarbon–benzene reaction, we monitored ion counts from $m/z = 113$ ($C_9H_5^+$) down to $m/z = 108$ (C_9^+). The TOFs at lower mass to charge ratios overlap with the patterns of the TOF recorded at $m/z = 113$. Therefore, signal in the range of $m/z = 112$ –108 originates in dissociative ionization of the parent molecule in the electron impact ionizer of the detector. Therefore, the tricarbon versus atomic hydrogen pathway is open (Fig. 1).

3.2. Center-of-mass functions

We would like to direct the discussion now to the derived center-of-mass translational energy distributions, $P(E_T)$ (Fig. 2). First, we can obtain information on the maximum translation energy of the reaction products in the center-of-mass frame. For the acetylene, ethylene, and benzene, best fits of the TOF and LAB data were achieved with a single channel fit and translational energy distributions extending up to 170 kJ mol^{-1} (acetylene), 120 kJ mol^{-1} (ethylene), and 75 kJ mol^{-1} (benzene). Secondly, all $P(E_T)$ s peak well away from zero translational energy at about 80 kJ mol^{-1} , 40 kJ mol^{-1} , and 25 kJ mol^{-1} ; the distributions depict a Gaussian-like shape. A comparison of these patterns with related reactions of carbon atoms [11] and dicarbon molecules with unsaturated hydrocarbon molecules suggests that a significant fraction of energy is being released into the translational degrees of freedom of the reaction products; most likely, the reaction also goes through short-lived reaction intermediates on the singlet C_5H_2 , C_5H_4 , and C_9H_6 and potential energy surfaces. It should be stressed that in order to get an acceptable fit of the data, it was important to include an energy-dependence of the reactive cross section via Eq. (1). Here, we varied the threshold energies between 10 and 150 kJ mol^{-1} . Best fits were derived for threshold energies between 80 and 90 kJ mol^{-1} , 40 and 50 kJ mol^{-1} ,

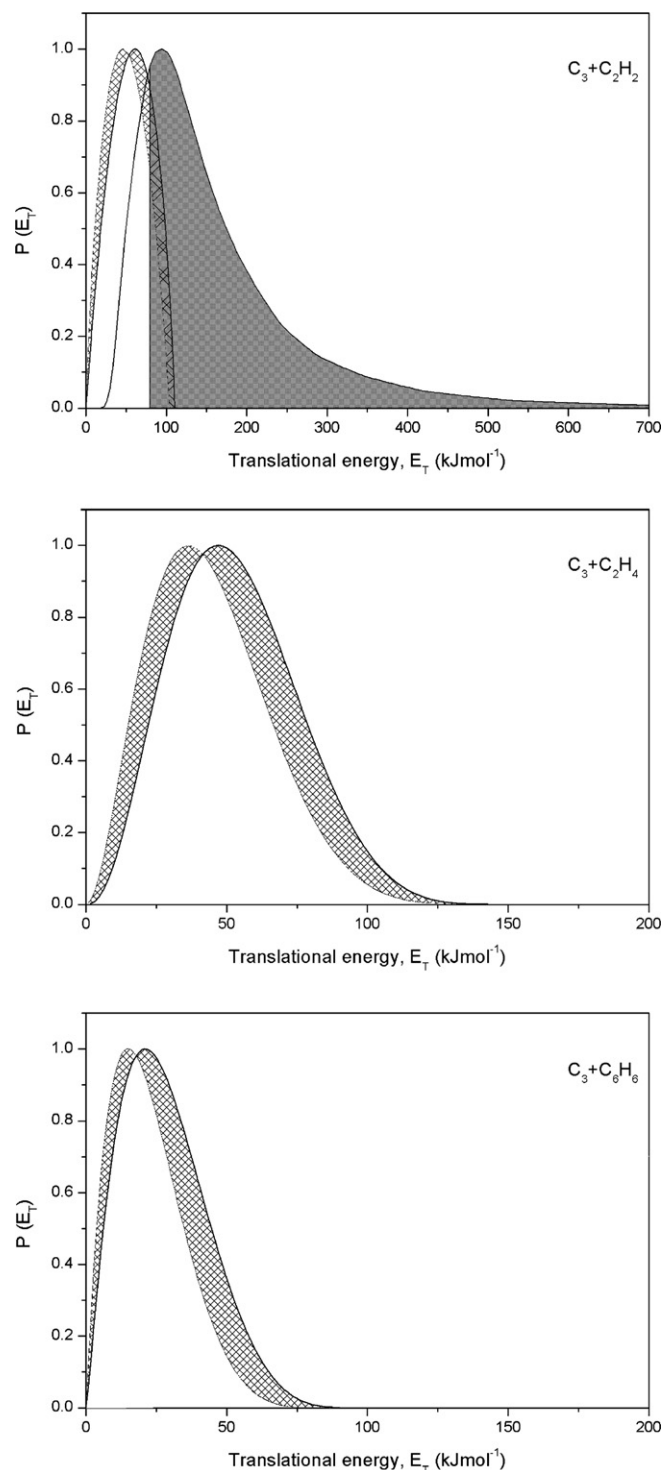


Fig. 2. Center-of-mass translational energy flux distributions for reaction of tricarbon with acetylene (top), ethylene (middle) and benzene (bottom) to form C_3H , C_5H_3 and C_9H_5 radical(s) and atomic hydrogen; the hatched areas comprise fits within the experimental error limits. In case of the acetylene and benzene systems, the distribution of collision energies is overlaid in gray.

and 90 and 110 kJ mol^{-1} for the acetylene, ethylene, benzene reactions, respectively.

It should be emphasized that the very narrow range of the reactive scattering signal as evident from the LAB dis-

tributions combined with the low speed ratio of the tricarbon beams make it problematical to derive quantitative information from the center-of-mass angular distributions, $T(\theta)$. Recall that to generate fast tricarbon beams, we have to utilize laser ablation of graphite and must select the early part of the ablation beam in which the tricarbon molecules are poorly helium-seeded [28]. This resulted in only limited speed ratios (Table 1). Unfortunately, there is currently no alternative to produce high velocity tricarbon beams (2900 ms⁻¹ and faster) except pulsed laser ablation. Based on the limited speed ratio, the fluctuations of the tricarbon beam velocity, and the narrow range of the reactive scattering signal, we cannot make a definite conclusions if the $T(\theta)$ s are forward or backward scattered with respect to the tricarbon beam. However, it is necessary to fit the data with intensity over the complete angular range from 0° to 180°; this suggests that the reactions are indirect and involve C₉H₆ intermediate(s). However, we can change the intensity ratios at the poles, $I(0^\circ)/I(180^\circ)$, from 4.0 to 0.2 in each system without having a significant effect on the fit.

4. Discussion

4.1. Energetics

To extract the underlying reaction dynamics, we would like to comment first on the energetics of the title reactions. Recall that the maximum translational energy of the center-of-mass translational energy distribution portrays the sum of the absolute of the reaction energy plus the collision energy. Therefore, by subtracting the latter, we find that in case of the ethylene and benzene systems, the reaction to form the C₅H₃ isomer(s) plus atomic hydrogen (ethylene reaction) and C₉H₅ isomer(s) plus atomic hydrogen (benzene reaction) is exoergic by about 47 ± 10 kJ mol⁻¹ (ethylene) and endoergic by about 100 ± 20 kJ mol⁻¹ (benzene). We can compare now the experimentally derived energetics with those obtained from calculations (Fig. 3) [22,23]. Here, the experimental data agree very well with the formation of the 1,2,3,4-pentatetraene-yl-1 radical, HCCCCCH₂(X²B₁) (ethylene) and of phenyltricarbon, C₆H₅CCC(X²A) – a species related to the recently identified 1,3-diphenylpropynylidene (C₆H₅CCCC₆H₅) [24] – in both cases, atomic hydrogen represents the co-product. Based on this information, we can also calculate the fraction of energy channeling on average into the translational modes of the reaction products to be about $50 \pm 5\%$ for both systems. This large fraction suggests that the reaction happens on a very short time scale [11].

The center-of-mass translational energy distribution of the reaction of tricarbon with acetylene to form C₅H + H presents a tricky problem. Based on the $P(E_T)$, we would derive an exoergicity of about 20 kJ mol⁻¹. However, a close look at the computed C₅H₂ potential energy surface (Fig. 3) indicates that the reaction to yield C₅H + H is endoergic by at least 100 kJ mol⁻¹. How can this obvious

discrepancy be accounted for? In Fig. 2, the $P(E_T)$ extracted from the tricarbon–acetylene reaction is overlaid by the distribution of collision energies. The latter has been computed from the peak velocities (v_p) and speed ratios (S) of the reactant beams. The effect of the limited speed ratio of the tricarbon beam and of the mass combinations of 61 amu (C₅H) plus 1 amu (H) is dramatic: we can see that energies up to a few 100 kJ mol⁻¹ present a significant fraction of this distribution. Therefore, we acknowledge that in case of the tricarbon–acetylene reaction, it is not feasible to provide reliable data on the reaction energies. As a matter of fact, the only firm information from the experimental data is the existence of a tricarbon versus atomic hydrogen channel and the presence of a characteristic threshold energy to reaction between 80 and 90 kJ mol⁻¹. Further, we can predict that the molecular hydrogen elimination pathway is closed. Also, since the collision energy in this system is extremely high (128 kJ mol⁻¹), we would anticipate a short life time of any intermediate involved. This is expected to prevent any hydrogen atom migrations [11] such as the isomerization from **i3** to **i5** and from **i1** to **i4** (Fig. 3). Note that the latter intermediate would be required if a molecular hydrogen elimination pathway was observed experimentally. These considerations correlate nicely with a recent theoretical study of this system [23]. Here, the authors predicted a dominating hydrogen elimination pathway to form the linear HCCCCC isomer; branching ratios for the molecular hydrogen channel plus pentacarbon were computed to be less than 0.7%. Due to the limitations on the experimental information on the tricarbon–acetylene system, the following paragraphs only discuss the possible dynamics of the tricarbon–ethylene and tricarbon–benzene reactions in depth.

4.1.1. Tricarbon–ethylene

We make an attempt now to resolve the underlying reaction dynamics leading to the synthesis of the 1,2,3,4-pentatetraene-yl-1 radical, HCCCCCH₂, by comparing our experimental findings with the computed potential energy surface (Fig. 3) [22]. We first correlate the structure of the tricarbon and ethylene reactants with the reaction product and suggest then feasible reaction intermediates on the singlet surface. Recall that although we could not extract quantitative information from the center-of-mass angular distribution, the experimental data indicate that the reactions must involve C₅H₄ reaction intermediates. Here, the carbon backbone in the 1,2,3,4-pentatetraene-yl-1 radical, HCCCCCH₂, is expanded by three carbon atoms compared to the ethylene reactant (H₂CCH₂). To connect the HCCCCCH₂ structure to the H₂CCH₂ reactant via C₅H₄ reaction intermediate(s), it is very likely that the reverse reaction, i.e. a hydrogen atom addition to the radical center at the CH group of the HCCCCCH₂ product forms a pentatetraene intermediate (H₂CCCCCH₂). To formally connect the H₂CCCCCH₂ intermediates with tricarbon plus ethylene, it is necessary to expand the carbon–carbon backbone by three carbon atoms. In a similar way

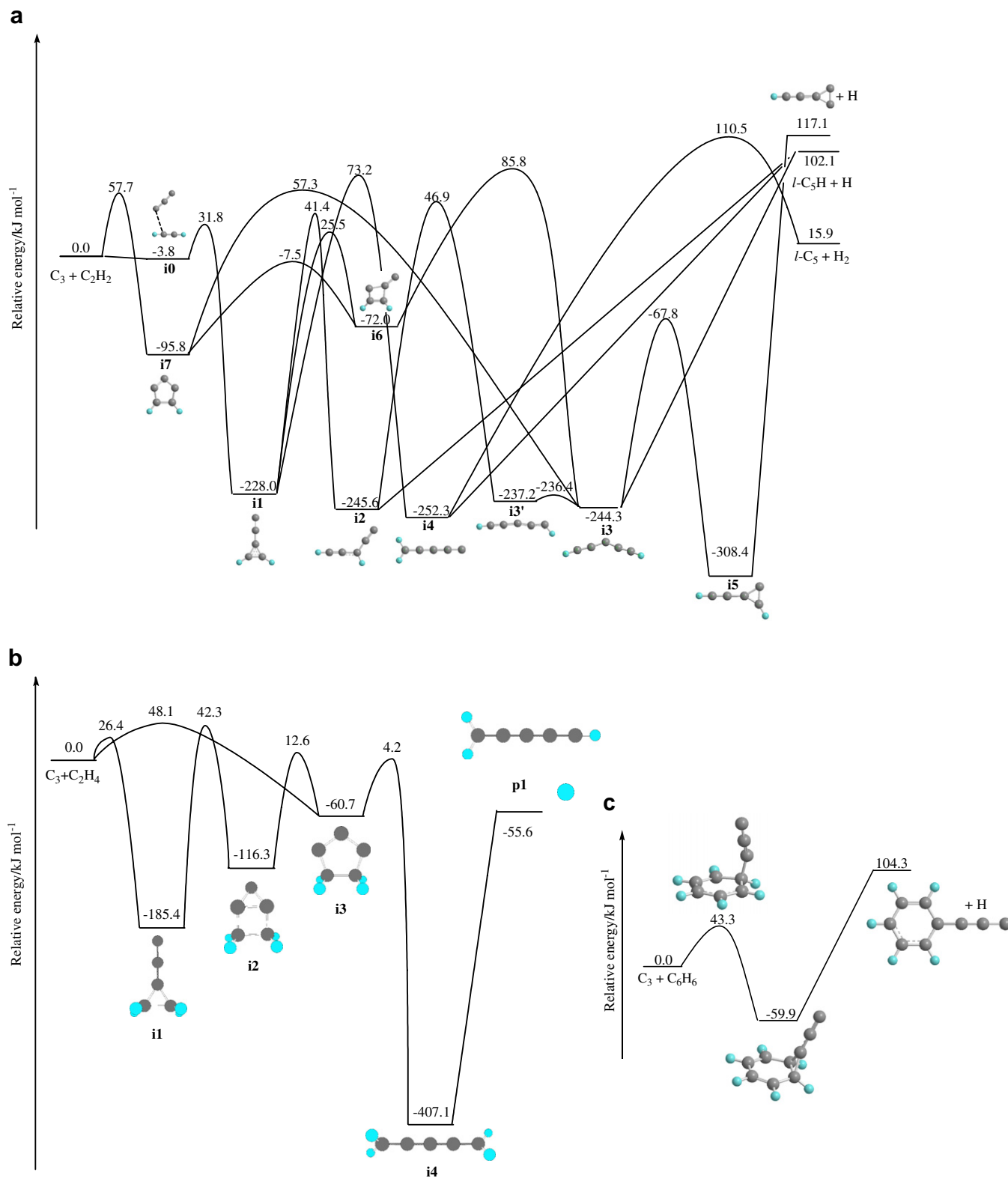


Fig. 3. Simplified potential energy surfaces involved in the reactions of tricarbon with acetylene (a), ethylene (b), and benzene (c).

to the reaction of singlet dicarbon with ethylene [14,21], we propose that the tricarbon reactant eventually ‘inserts’ into the carbon–carbon double bond of the ethylene molecule. Since it is not feasible for the tricarbon reactant to ‘insert’ in a single step, we propose that tricarbon adds to the

carbon–carbon double bond of the ethylene reactant to form initially cyclic C_5H_4 collision complex(es) on the singlet surface. Based on our experiment, this process was found to have a characteristic threshold energy of 40–50 kJ mol⁻¹. The initial cyclic reaction intermediate(s)

can isomerize to form eventually the pentatetraene intermediate ($\text{H}_2\text{CCCCCH}_2$).

The computations confirm this postulated reaction mechanism (Fig. 3) [22]. Here, tricarbon can add in one step either side on or end-on to the carbon–carbon double bond forming the intermediates **i3** and **i1**, respectively. Both addition processes have characteristic entrance barriers of about 26 and 48 kJ mol^{-1} . Intermediate **i1** can rearrange stepwise via **i2** to **i3**. Ultimately, **i3** ring opens to form the postulated pentatetraene intermediate **i4** ($\text{H}_2\text{CCCCCH}_2$) on the singlet surface. However, the computed surface suggests that the pentatetraene molecule loses a hydrogen atom via a loose exit transition state, i.e. a simple bond rupture process. This should be reflected in a center-of-mass translational energy distribution peaking at or close to zero translational energy. This is clearly not observed (Fig. 2). How can this be explained? The large fraction of the available energy channeling into the translational degrees of freedom of about 50% suggest that the decomposing intermediate is very short-lived – possible at the borderline between direct and indirect dynamics. Considering the large collision energy, this finding is not surprising. The very short life time can result in the experimentally observed off-zero peaking of the center-of-mass translational energy distributions. Previous crossed beam experiments, of for instance electronically excited carbon atoms with acetylene [25], ethylene, and propylene [26] at high collision energies of at least 45 kJ mol^{-1} showed explicitly that – although the decomposing intermediates formally reside in deep potential energy wells – the translational energy distributions peak well away from zero translational energy. Therefore, our data of the ethylene–tricarbon experiment indicate the presence of a short-lived $\text{H}_2\text{CCCCCH}_2$ intermediate decomposing rather ‘directly’ than via a long-lived complex behavior.

4.1.2. Tricarbon–benzene

To propose the underlying reaction dynamics, we follow a similar approach as utilized in the tricarbon–ethylene reaction and compare our experimental data with the computed potential energy surface (Fig. 2). In our calculations, the reactants, products, intermediates, and transition states on the relevant part of the C_9H_6 potential energy surface for the $\text{C}_3(\text{X}^1\Sigma_g^+)$ plus benzene reactions were optimized using the hybrid density functional B3LYP method with the 6-311G(d,p) basis set [27,28]. Vibrational frequencies were computed at the same level of theory for the characterization of stationary points and to obtain zero-point energy (ZPE) corrections. More accurate relative energies were recalculated using the G3(MP2,CCSD)//B3LYP method [29], which approximates the coupled cluster [30] CCSD(T)/G3MP2 large energy. All calculations were carried out using the GAUSSIAN 98 [31] and MOLPRO 2000 [32] programs. Because the average absolute deviation of the G3(MP2,CCSD)//B3LYP method for enthalpies of formation in the G3 molecular test set is 5 kJ mol^{-1} , we expect that our calculations of relative energies are

accurate to $\pm 10 \text{ kJ mol}^{-1}$. Having identified phenyltricarbon, $\text{C}_6\text{H}_5\text{CCC}$, as the reaction product, we now connect the molecular structures of the tricarbon and benzene reactants with the reaction product. Formally, a carbon atom of the benzene molecule is replaced by the tricarbon molecular unit. This exchange is similar to the reactions of, for instance, the reactions of singlet dicarbon benzene leading to the phenylethynyl radical ($\text{C}_6\text{H}_5\text{CC}$). Here, we propose that tricarbon attacks the aromatic ring leading to a $\text{C}_6\text{H}_6\text{CCC}$ intermediate; the latter may lose a hydrogen atom to form the phenyltricarbon radical ($\text{C}_6\text{H}_5\text{CCC}$).

The computations of the relevant parts of the C_9H_6 potential energy surface support the proposed reaction mechanism (Fig. 3) [22]. Here, tricarbon can add to the aromatic ring via an entrance barrier to yield a weakly bound bicyclic intermediate stabilized by about 60 kJ mol^{-1} [33]. Vala and coworkers calculated this intermediate to lie 52 and 46 kJ mol^{-1} below the reactants at the less accurate density functional B3LYP level with the 6-31G** and 6-311+G** basis sets, respectively. They also found weakly bound π -complexes of tricarbon with benzene stabilized by 8 kJ mol^{-1} between the reactants and the bicyclic intermediate. The transition state leading to this intermediate from tricarbon plus benzene (via the π -complexes) is located 43 kJ mol^{-1} above the reactants at our G3(MP2,CCSD) level, somewhat lower than 54 kJ mol^{-1} obtained in B3LYP calculations [33]. Vala and coworkers also considered various isomerization pathways of the bicyclic C_9H_6 intermediate, which are apparently not relevant to the hydrogen atom elimination reaction leading to the $\text{C}_6\text{H}_5\text{CCC}$ product identified in our experiment. We have found here that, accompanied by a three-member ring opening, the bicyclic intermediate emits a hydrogen atom to synthesize the phenyltricarbon radical. The overall reaction to form phenyltricarbon plus atomic hydrogen was found to be endoergic by 104 kJ mol^{-1} . This value correlates nicely with the experimentally derived energetics and also with the observed reaction threshold of 90–110 kJ mol^{-1} . In a similar manner to the tricarbon–ethylene system, the surface indicates that the intermediate should emit the hydrogen atom via a loose exit transition state. This is expected to result in a center-of-mass translational energy distribution peaking at or close to zero translational energy. Again, this is not observed (Fig. 2). Here, the significant fraction of the available energy channeling into the translational degrees of freedom of about 50% indicates that the fragmenting intermediate is short-lived. Also, considering the large collision energy, this finding is not surprising, and dynamical effects likely result in the observed off-zero peaking of the center-of-mass translational energy distributions.

5. Summary

In our crossed beams experiments, we investigated the reaction of tricarbon molecules, $\text{C}_3(\text{X}^1\Sigma_g^+)$, with acetylene

(C₂H₂), ethylene (C₂H₄), and benzene (C₆H₆). The experiments suggested that all reactions proceeded via a tricarbon versus atomic hydrogen exchange pathway. Further, the reactions were characterized by threshold energies, E_0 , of 80–90 kJ mol⁻¹, 40–50 kJ mol⁻¹, and 90–110 kJ mol⁻¹. In case of the acetylene reactant, it was not feasible to derive detailed dynamical information on the tricarbon–acetylene reaction on the experiments alone. However, the tricarbon–ethylene and tricarbon–benzene reactions were found to proceed via initial addition processes of the tricarbon molecule to the unsaturated hydrocarbon on the singlet surfaces. In case of ethylene, the cyclic intermediates isomerized to yield eventually the acyclic pentatetraene intermediate (H₂CCCCCH₂). The actual lifetime of this intermediate is proposed to be rather short; it was found to decompose via atomic hydrogen elimination to form the 1,2,3,4-pentatetraene-yl-1 radical, HCCCCCH₂(X²B₁). Note that the experimentally derived threshold energy of the tricarbon–ethylene reaction is similar as found for the reaction of tricarbon with allene and methylacetylene, i.e. 40–50 kJ mol⁻¹. Together with the endoergic reaction of tricarbon with benzene and acetylene, these data can rationalize now the low rate constants of less than 10⁻¹² cm³ s⁻¹ derived previously in kinetics studies of these reactions [7]. This is in strong contrast to the reactions of dicarbon molecules with unsaturated hydrocarbons acetylene, ethylene, benzene, methylacetylene, and allene, which have no entrance barrier [14]. The different reactivities of singlet dicarbon and tricarbon could be rationalized in distinct HOMO–LUMO gaps of 171 and 444 kJ mol⁻¹, respectively, at the B3LYP/6-311G** level. Also, dicarbon possesses low-lying excited electronic states, as the a³Π_u, b³Σ_g⁻, and A¹Π_u states are only 8.6, 77.0, and 100.4 kJ mol⁻¹ higher in energy than the ground X¹Σ_g⁺ state, respectively. On the contrary, the lowest excited triplet and singlet states of acyclic tricarbon molecule lie 202.5 and 293.1 kJ mol⁻¹ above the ground electronic state [34]. The much wider HOMO–LUMO gap and the absence of low-lying excited states for C₃ explain its significantly lower reactivity as compared to dicarbon.

The existence of reaction thresholds on bimolecular reactions of tricarbon molecules with unsaturated hydrocarbons has important implications to combustion and interstellar chemistry. Our findings suggest that tricarbon molecules can certainly react in high temperature combustion flames with unsaturated hydrocarbon molecules to form hydrogen-deficient, often resonantly stabilized free radicals; the latter can be important intermediates in the formation of soot particles. But the inherent barriers certainly prevent any reactions of tricarbon molecules – at least with unsaturated hydrocarbons – in cold molecular clouds where average translation temperatures of about 10 K exist. However, extraterrestrial settings like regions of circumstellar envelopes like IRC +10216 close to the central stars and interstellar shocks where translational temperatures can reach up to a few 1000 K could support tricarbon reactions.

Acknowledgements

The work was supported by the US Department of Energy-Basic Energy Sciences (DE-FG02-03ER15411 (RIK) and DE-FG02-04ER15570 (AMM)).

References

- [1] Faraday Discussion 119, Combustion Chemistry: Elementary Reactions to Macroscopic Processes, 2001.
- [2] P. John, J.R. Rabeau, J.I.B. Wilson, *Diam. Relat. Mater.* 11 (2002) 608.
- [3] A.G. Gordon, *The Spectroscopy of Flames*, Chapman and Hall Ltd., Wiley, New York, 1974.
- [4] T. Shiomi, H. Nagai, K. Kato, M. Hiramatsu, M. Nawata, *Diam. Relat. Mater.* 10 (2001) 388.
- [5] S.A. Redman, C. Chung, K.N. Rosser, M.N.R. Ashfold, *Phys. Chem. Chem. Phys.* 1 (1999) 1415; J.S. Foord, K.P. Loh, N.K. Singh, R.Z.B. Jackman, G.J. Davies, *J. Cryst. Growth* 164 (1996) 208.
- [6] A.G. Loewe, A.T. Hartlieb, J. Brand, B. Atakan, K. Kohse-Hoeinghaus, *Combust. Flame* 118 (1999) 37.
- [7] H.H. Nelson, L. Pasternack, J.R. Eyler, J.R. McDonald, *Chem. Phys.* 60 (1981) 231; M.L. Lesiecki, K.W. Hicks, A. Orenstein, W.A. Guillory, *Chem. Phys. Lett.* 71 (1980) 72.
- [8] H.H. Nelson, H. Helvajian, L. Pasternack, J.R. McDonald, *Chem. Phys.* 73 (1982) 431. <<http://kinetics.nist.gov/index.php>>.
- [9] K. Liu, *J. Chem. Phys.* 125 (2006) 132307.
- [10] N. Balucani, G. Capozza, F. Leonori, E. Segoloni, P. Casavecchia, *Int. Rev. Phys. Chem.* 25 (2006) 109.
- [11] R.I. Kaiser, *Chem. Rev.* 102 (2002) 1309.
- [12] Y. Guo, X. Gu, F. Zhang, A.M. Mebel, R.I. Kaiser, *Phys. Chem. Chem. Phys.* 9 (2007) 1972.
- [13] X. Gu, Y. Guo, A.M. Mebel, R.I. Kaiser, *J. Phys. Chem. A* 110 (2006) 11265.
- [14] X. Gu, Y. Guo, F. Zhang, A.M. Mebel, R.I. Kaiser, *Faraday Discuss.* 133 (2006) 245.
- [15] X. Gu, Y. Guo, E. Kawamura, R.I. Kaiser, *J. Vac. Sci. Technol. A* 24 (2006) 505.
- [16] X. Gu, Y. Guo, H. Chan, E. Kawamura, R.I. Kaiser, *Rev. Sci. Instr.* 76 (2005) 116103.
- [17] M.S. Weiss, PhD Thesis, University of California, Berkeley, CA, 1986; M. Vernon, PhD Thesis, University of California, Berkeley, CA, 1981; R.I. Kaiser, C. Ochsenfeld, D. Stranges, M. Head-Gordon, Y.T. Lee, *Faraday Discuss.* 109 (1998) 183.
- [18] R.D. Levine, *Molecular Reaction Dynamics*, Cambridge University Press, Cambridge, 2005.
- [19] X. Gu, Y. Guo, R.I. Kaiser, *Int. J. Mass Spectrom.* 261 (2007) 100.
- [20] R.I. Kaiser, C. Ochsenfeld, M. Head-Gordon, Y.T. Lee, A.G. Suits, *J. Chem. Phys.* 106 (1997) 1729.
- [21] N. Balucani, A.M. Mebel, Y.T. Lee, R.I. Kaiser, *J. Phys. Chem. A* 43 (2001) 9813.
- [22] R.I. Kaiser et al., *Faraday Discuss.* 119 (2001) 51.
- [23] A.M. Mebel, G.-S. Kim, V.V. Kislov, R.I. Kaiser, *J. Phys. Chem. A* 111 (2007) 6704.
- [24] J.T. DePinto, W.A. deProphetis, J.L. Menke, R.J. McMahon, *J. Am. Chem. Soc.* 129 (2007) 2308.
- [25] R.I. Kaiser, A.M. Mebel, Y.T. Lee, *J. Chem. Phys.* 114 (2001) 231.
- [26] R.I. Kaiser, T.L. Nguyen, A.M. Mebel, Y.T. Lee, *J. Chem. Phys.* 116 (2002) 1318.
- [27] A.D. Becke, *J. Chem. Phys.* 98 (1993) 5648.
- [28] C. Lee, W. Yang, R.G. Parr, *Phys. Rev. B* 37 (1988) 785.

- [29] L.A. Curtiss, K. Raghavachari, P.C. Redfern, A.G. Baboul, J.A. Pople, *Chem. Phys. Lett.* 314 (1999) 101.
- [30] G.D. Purvis, R.J. Bartlett, *J. Chem. Phys.* 76 (1982) 1910.
- [31] M.J. Frisch et al., *GAUSSIAN 98*, Revision A.7 Gaussian, Inc., Pittsburgh PA, 1998.
- [32] MOLPRO is a package of ab initio programs written by H.-J. Werner, P.J. Knowles with contributions from J. Almlöf, R.D. Amos, M.J.O. Deegan, S.T. Elbert, C. Hampel, W. Meyer, K. Peterson, R. Pitzer, A.J. Stone, P.R. Taylor, R. Lindh.
- [33] J. Szczepanski, H. Wang, M. Vala, *Chem. Phys.* 303 (2004) 165.
- [34] NIST Chemistry Webbook, NIST Standard Reference Data Base Number 69, June 2005 Release. <<http://webbook.nist.gov/chemistry>>.